RESEARCH ARTICLE

Two-Electron Redox Reactivity of Thorium Supported by Redox-Active Tripodal Frameworks

Fang-Che Hsueh,[a] Damien Chen,[a] Thayalan Rajeshkumar,[c] Rosario Scopelliti,[b] Laurent Maron,[c] and Marinella Mazzanti*[a]

[a] F.-C. Hsueh, D. Chen, Prof. M. Mazzanti
Group of Coordination Chemistry, Institut des Sciences et Ingénierie Chimiques, École Polytechnique Fédérale de Lausanne (EPFL), 1015, Lausanne, Switzerland. Email: marinella.mazzanti@epfl.ch.

[b] Dr. R. Scopelliti, Institut des Sciences et Ingénierie Chimiques, École Polytechnique Fédérale de Lausanne (EPFL), 1015, Lausanne, Switzerland.

[c] T. Rajeshkumar, Prof. L. Maron
Laboratoire de Physique et Chimie des Nano-objets, Institut National des Sciences Appliquées, 31077 Toulouse, Cedex 4, France

Abstract: The high stability of the +4 oxidation state limits thorium redox reactivity. Here we report the synthesis and the redox reactivity of two Th(IV) complexes supported by the arene-tethered tris(siloxide) tripodal ligands [(KOSiR_2Ar)$_3$-arene)]. The two electron reduction of these Th(IV) complexes generates the doubly reduced [KTh((OSi(O^{t}Bu)$_2$Ar)$_3$-arene)(THF)$_2$] (**2^{OtBu}**) and [K(2.2.2-cryptand)][Th(OSiPh$_2$Ar)$_3$-arene)(THF)$_2$](**2^{Ph}-crypt**) where the formal oxidation state of Th is +II. Structural and computational studies indicate that the reduction occurred at the arene anchor of the ligand. The robust tripodal frameworks store in the arene anchor two electrons that become available at the metal center for the two-electron reduction of a broad range of substrates (N_2O, COT, CHT, Ph_2N_2, Ph_3PS and O_2) while retaining the ligand framework. This work shows that arene-tethered tris(siloxide) tripodal ligands allow implementation of two-electron redox chemistry at the thorium center while retaining the ligand framework unchanged.

Introduction

Recent research in uranium chemistry allowed expansion of the number of accessible oxidation states (+I to +VI) with the discovery of molecular compounds of uranium in +I[1] and +II[2],[3a, 3b, 2d, 3c] oxidation state. Moreover, the ability of uranium to engage in multielectron transfer[4] reactions enabled the reduction of small unreactive molecules such as dinitrogen[5] or carbon dioxide.[6] In contrast, the chemistry of thorium remains mainly limited to one oxidation state (+IV)[7], with only few examples of compounds of thorium in the +II and +III oxidation state. [8] The high stability of Th(IV) and the tendency of Th(II) and Th(III) to undergo decomposition and disproportionation reactions has hindered the development of thorium redox chemistry.[9] Alternatively, multi-electron transformations of metal centers with low redox flexibility can be enabled by using redox-active ligands, but the use of redox-active ligands to enable multi-electron transformations remains rare in thorium chemistry.[10], [11]

Arenes and arenides are a class of redox-active ligands increasingly studied in f element chemistry.[12a-g, 4k, 12h-p] Arenide complexes of thorium were reported twenty years ago,[11] but only recently arenides have attracted renewed interest in thorium chemistry as redox-active supporting ligands.[12o, 3c, 13] Notably we recently showed that a mononuclear arenide complex and an Inverse-sandwich complex of thorium can perform multielectron reductive chemistry with a range of substrates, acting as Th(II) synthons.[13] However, loss of the arenide ligand during reactivity limits these systems versatility. Stabilization of unusual oxidation states and more controlled multielectron transfer reactivity were achieved in uranium[3a, 4k, 14] and in cerium chemistry[15] using an arene anchor to tether aryloxide, amide or siloxide ligands. However, such arene-anchored tripodal ligand were never used in thorium chemistry. Here we report the synthesis and the redox reactivity of two Th(IV) complexes supported by arene-tethered tris(siloxide) tripodal ligands [(KOSiR_2Ar)$_3$-arene)] (R= O^{t}Bu[15a] or Ph[16]). The robust tripodal frameworks store electrons that become available at the metal center for the two-electron reduction of substrates while retaining the ligand framework.

Results and Discussion

At first, we pursued the synthesis of two heteroleptic Th(IV) complexes with arene-tethered tris(siloxide) tripodal ligands presenting different substituents, [ThCl((OSiR_2Ar)$_3$-arene)(THF)$_x$] (**1^{OtBu}**: R= O^{t}Bu, x= 1, **1^{Ph}**: R= Ph, x= 2)(Scheme 1).

Addition of 1.0 equiv. of ligand salt [(KOSiR_2Ar)$_3$-arene)] (R= O^{t}Bu or Ph) to 1.0 equiv. of [ThCl$_4$(DME)$_2$] in THF at room temperature, resulted in a white suspension. After 16 hours, the formation of new species and full consumption of ligand salt [(KOSiR_2Ar)$_3$-arene)] (R= O^{t}Bu or Ph) was observed by ^{1}H NMR spectroscopy (Figure S4 and S14). Colorless crystals of complexes **1^{OtBu}** and **1^{Ph}** were isolated at -40 °C in 90% and 89% yield from a concentrated toluene and a concentrated THF/Hexane solution, respectively. The ^{1}H NMR spectrum of the isolated complex **1^{OtBu}** revealed five resonances at δ 2.56, 3.02, 3.72, 4.90, and 10.68 ppm, which correspond to the –OSi(O^{t}Bu)$_2$ and tripodal arene moieties. Similarly, the ^{1}H NMR spectrum of isolated complex **1^{Ph}** shows five resonances at δ 6.79, 7.04, 7.06-7.24, 7.54, and 7.73 ppm, corresponding to the –OSiPh$_2$ and tripodal arene moieties. Significant differences were observed in the ^{29}Si{^{1}H} NMR resonances (δ -75.45 ppm for –OSi(O^{t}Bu)$_2$ and δ -22.04 ppm for –OSiPh$_2$) in complexes **1^{OtBu}** and **1^{Ph}** due to the stronger electron-donating character of the phenyl substituents. The solid-state molecular structures of complexes **1^{OtBu}** and **1^{Ph}** were determined by X-ray diffraction studies.

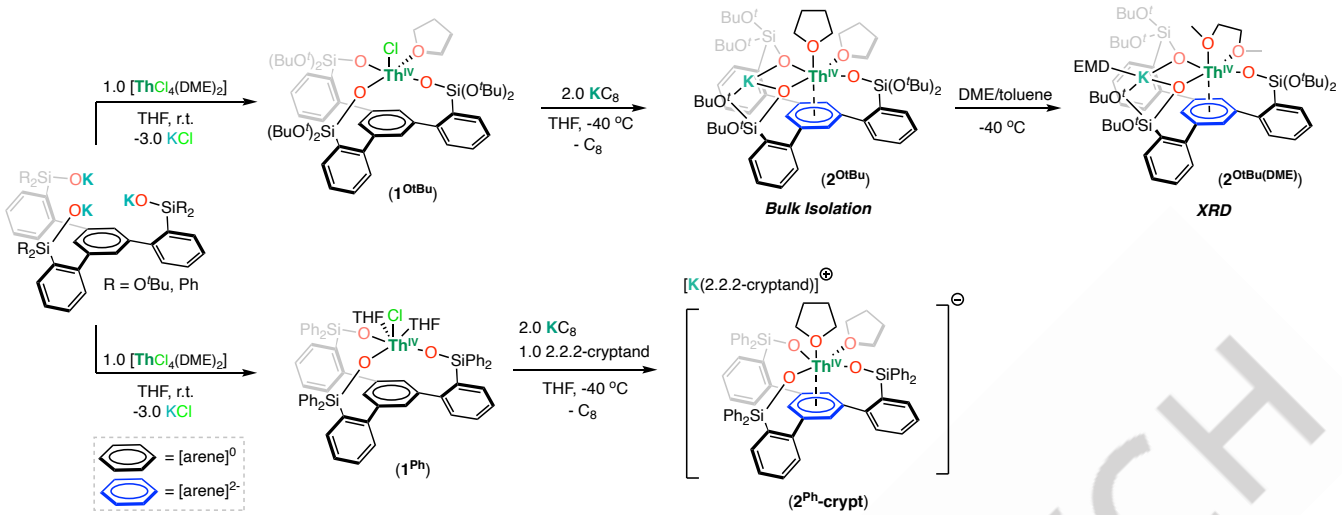

Scheme 1. Synthesis of complexes $\mathbf{1}^{\mathbf{OtBu}}$, $\mathbf{1}^{\mathbf{Ph}}$, $\mathbf{2}^{\mathbf{OtBu}}$, $\mathbf{2}^{\mathbf{OtBu(DME)}}$ and $\mathbf{2}^{\mathbf{Ph}}$**-crypt** supported by trianionic tripodal ligands.

The molecular structures of complexes $\mathbf{1}^{\mathbf{OtBu}}$ and $\mathbf{1}^{\mathbf{Ph}}$ and selected structural parameters are presented in Figure 1 and Table 1.

Both structures show the presence of Th(IV) ions coordinated by the tripodal ligands and an axial chloride ligand, along with THF ligands, but display different coordination geometries. In complex $\mathbf{1}^{\mathbf{OtBu}}$ the Th(IV) center is penta-coordinated by three –OSi(O^{t}Bu)$_2$ groups of the tripodal ligand, one axial chloride ligand, and one coordinated THF, with a distorted square pyramidal geometry. In contrast, in complex $\mathbf{1}^{\mathbf{Ph}}$ the Th(IV) is hexa-coordinated, having two coordinated THF ligands instead of one as found in $\mathbf{1}^{\mathbf{OtBu}}$, and adopts a distorted octahedral arrangement. This difference is most likely due to the higher steric crowding provided by the di-*tert*-butylsiloxide compared to the diphenylsiloxide. The average Th-O$_{siloxide}$ distances in both complexes are comparable, with $\mathbf{1}^{\mathbf{OtBu}}$ exhibiting an average value of 2.180(3) Å and $\mathbf{1}^{\mathbf{Ph}}$ showing a similar value of 2.176(12) Å. The Th-arene distance in $\mathbf{1}^{\mathbf{OtBu}}$ (Th-C$_{centroid}$ =3.1508(13) Å) is significantly shorter than that found in $\mathbf{1}^{\mathbf{Ph}}$ (Th-C$_{centroid}$ =4.070(4) Å), but in both cases the Th-arene distance is longer than those found in other Th(IV) neutral arene complexes (Th-centroid distances ranging from 2.619 to 2.95 Å)[17] suggesting the presence of very weak Th-arene interactions with significantly weaker interactions in $\mathbf{1}^{\mathbf{Ph}}$ when compared to $\mathbf{1}^{\mathbf{OtBu}}$. Moreover, the average C-C bond length in the centroid arene of $\mathbf{1}^{\mathbf{OtBu}}$ (1.400(6) Å) is slightly longer than that found in $\mathbf{1}^{\mathbf{Ph}}$ (1.389(6) Å) but remains comparable to that found in the free ligand [(HOSiPh$_2$Ar)$_3$-arene)] (1.3932(19) Å),[16b] further emphasizing the lack of significant thorium-arene interactions in both complexes. Meanwhile, the Th-Cl distance in $\mathbf{1}^{\mathbf{Ph}}$ (2.728(2) Å) is slightly longer than that in $\mathbf{1}^{\mathbf{OtBu}}$ (2.6628(10) Å, but remains comparable to that found in the previously reported Th(IV) complex [Th(OSi(O^{t}Bu)$_3$)$_3$Cl(THF)$_2$] (2.735(3) Å).[18]

With these tripodal ThCl complexes $\mathbf{1}^{\mathbf{OtBu}}$ and $\mathbf{1}^{\mathbf{Ph}}$ in hand, we set out to investigate if $\mathbf{1}^{\mathbf{OtBu}}$ and $\mathbf{1}^{\mathbf{Ph}}$ could be reduced and to compare their redox reactivity (Scheme 1).

The reaction of $\mathbf{1}^{\mathbf{OtBu}}$ with 1.0 equiv. of KC$_8$ in THF at -40°C resulted in a mixture of $\mathbf{1}^{\mathbf{OtBu}}$ and of a new species, $\mathbf{2}^{\mathbf{OtBu}}$, as observed by ^{1}H NMR spectroscopy (Figure S8). The addition of a second equiv. of KC$_8$ to the reaction mixture at -40°C led to a full consumption of $\mathbf{1}^{\mathbf{OtBu}}$ and a clean formation of a new species as indicated by ^{1}H NMR spectroscopy (Figure S8). Similarly, the reduction of $\mathbf{1}^{\mathbf{Ph}}$ also requires 2.0 equiv. of KC$_8$ for the full consumption of $\mathbf{1}^{\mathbf{Ph}}$, yielding a new species, $\mathbf{2}^{\mathbf{Ph}}$, as confirmed by ^{1}H NMR spectroscopy (Figure S18). The di-reduced complex [KTh((OSi(O^{t}Bu)$_2$Ar)$_3$-arene)(THF)$_2$] ($\mathbf{2}^{\mathbf{OtBu}}$) was isolated from a mixture of THF and n-hexane at -40 °C in 89% yield. Attempts to obtain X-ray suitable single crystals of the $\mathbf{2}^{\mathbf{OtBu}}$ were unsuccessful. However, a few dark red-brown crystals suitable for X-ray crystallography analysis of the complex [K(DME)Th((OSi(O^{t}Bu)$_2$Ar)$_3$-arene)(DME)] ($\mathbf{2}^{\mathbf{OtBu(DME)}}$) were isolated from a concentrated DME/toluene mixture at -40 °C. On the other hand, attempts to obtain X-ray suitable single crystals of the $\mathbf{2}^{\mathbf{Ph}}$ from the reduction of $\mathbf{1}^{\mathbf{Ph}}$ were unsuccessful.

However, upon the addition of 1.0 equiv. of 2.2.2-cryptand and 2.0 equivalents of KC$_8$ to $\mathbf{1}^{\mathbf{Ph}}$ at -40 °C, a new set of resonances appeared in the ^{1}H NMR spectrum (Figure S20) recorded at room temperature. Eventually, dark purple crystals of complex [K(2.2.2-cryptand)][Th(OSiPh$_2$Ar)$_3$-arene)(THF)$_2$]($\mathbf{2}^{\mathbf{Ph}}$**-crypt**) were obtained from a concentrated THF/*n*-hexane mixture at -40 °C in 92% yield. Moreover, adding 1.3 equiv. of 2.2.2-cryptand to $\mathbf{2}^{\mathbf{Ph}}$ led to the formation of $\mathbf{2}^{\mathbf{Ph}}$**-crypt** as observed by ^{1}H NMR spectroscopy (Figure S19).

The solid-state molecular structure of complex $\mathbf{2}^{\mathbf{OtBu(DME)}}$ and $\mathbf{2}^{\mathbf{Ph}}$**-crypt** were determined by X-ray diffraction studies (Figure 1 and Table 1). The molecular structure of $\mathbf{2}^{\mathbf{OtBu(DME)}}$ shows the presence of a neutral complex where the K$^+$ cation is bound by two siloxide arms of the [K(DME)Th((OSi(O^{t}Bu)$_2$Ar)$_3$-arene)(DME)] moiety and one coordinated DME. The structure of $\mathbf{2}^{\mathbf{Ph}}$**-crypt** shows the presence of an ion pair consisting of one outer sphere [K(2.2.2-cryptand)]$^+$ cation and the [Th(OSiPh$_2$Ar)$_3$-arene)(THF)$_2$]$^-$ anion.

The Th center in $\mathbf{2}^{\mathbf{OtBu(DME)}}$ and $\mathbf{2}^{\mathbf{Ph}}$**-crypt** is coordinated by the three siloxide groups of the tripodal ligand, the distorted arene anchor and one DME (in $\mathbf{2}^{\mathbf{OtBu(DME)}}$) or two THF (in $\mathbf{2}^{\mathbf{Ph}}$**-crypt**) molecules. The average value of the Th-O$_{siloxide}$ bond lengths in

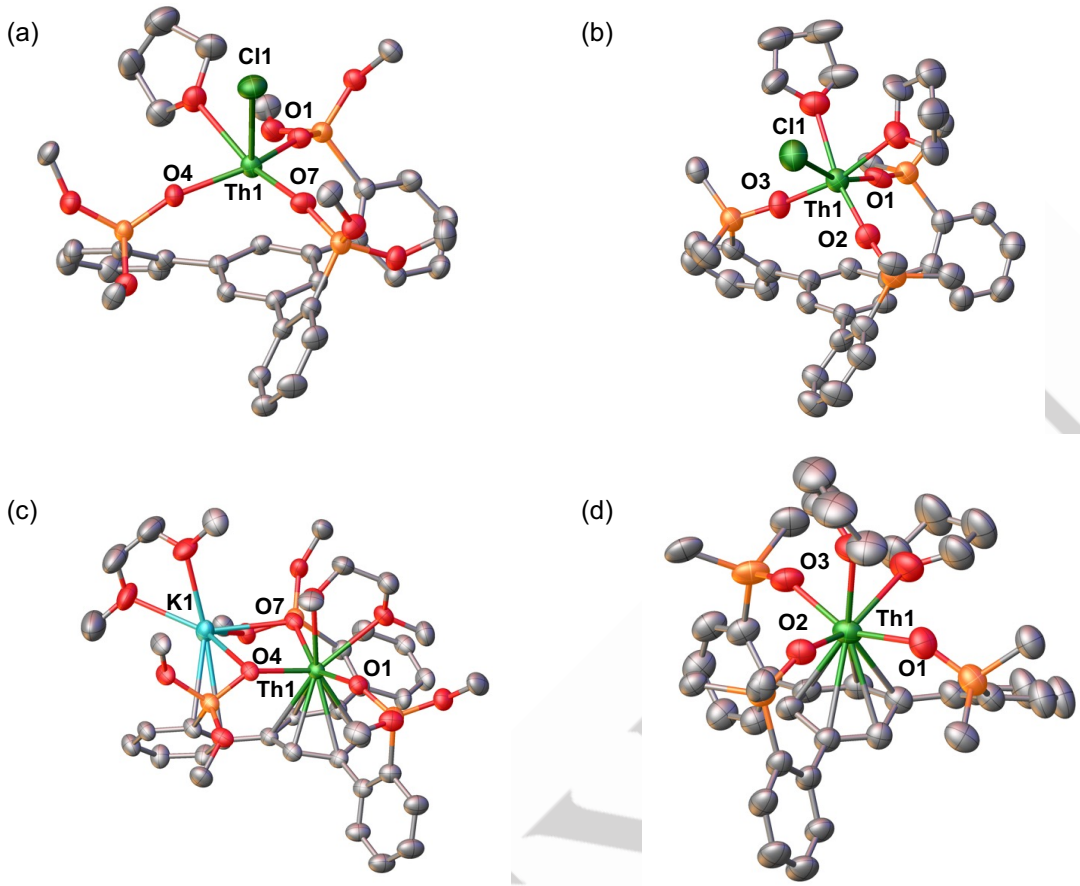

Figure 1. Molecular structures of (a) [ThCl((OSi(O^{t}Bu)$_2$Ar)$_3$-arene)(THF)], **1^{OtBu}**, (b) [ThCl((OSiPh$_2$Ar)$_3$-arene)(THF)$_2$], **1^{Ph}**, (c) [K(DME)Th((OSi(O^{t}Bu)$_2$Ar)$_3$-arene)(DME)], **2$^{OtBu(DME)}$**, (d) [K(2.2.2-cryptand)][Th(OSiPh$_2$Ar)$_3$-arene)(THF)$_2$], **2^{Ph}-crypt** with thermal ellipsoids at drawn at the 50% probability level. Hydrogen atoms, methyl groups on the –OSi(O^{t}Bu)$_2$ ligands, [K(2.2.2-cryptand)]$^+$ and five carbon atoms of each Ph group have been omitted for clarity.

Table 1. Selected bond lengths (Å) and angles (°) for complexes **1^{OtBu}**, **1^{Ph}**, **2$^{OtBu(DME)}$** and **2^{Ph}-crypt**.

Complex	**1^{OtBu}**	**1^{Ph}**	**2$^{OtBu(DME)}$**	**2^{Ph}-crypt**
Th–O$_{siloxide}$	2.175(3)-2.184(3)	2.160(6)-2.190(6)	2.285(10)-2.332(11)	2.257(3)-2.298(3)
Th–Cl	2.6628(10)	2.728(2)	--	--
Th–C$_{arene}$	--	--	2.647(16)-2.848(16)	2.623(5)-2.866(5)
Th–C$_{centroid}$	3.1508(13)	4.070(4)	2.364(8)	2.3869(19)
C–C$_{arene}$	1.391(5)-1.409(5)	1.382(12)-1.399(11)	1.36(2)-1.50(2)	1.359(8)-1.499(7)
Torsion angles (central arene)	0.4(4)-2.3(3)°	0.1(13)-4.2(13)°	7(2)-21(2)°	1.7(8)-24.5(7)°

the reduced complexes **2$^{OtBu(DME)}$** (2.29(3) Å) and **2^{Ph}-crypt** (2.2824(18) Å) increases compared to those found in precursors, **1^{OtBu}** (2.180(3) Å) and **1^{Ph}** (2.176(12) Å). These distances are comparable to those found in the recently reported thorium arenide complexes supported by –OSi(O^{t}Bu)$_3$, [K(OSi(O^{t}Bu)$_3$)$_3$Th(η^6-C$_{10}$H$_8$)] (2.238(5) Å).[13] The range of O-Th1-O bond angles found in the reduced complexes **2$^{OtBu(DME)}$** (91.8(4)-150.4(4)°) and **2^{Ph}-crypt** (90.23(13)-151.53(14)°) are larger than those found in the precursors, **1^{OtBu}** (106.24(10)-140.44(10)°) and **1^{Ph}** (95.6(2)-106.2(2)°) respectively. Notably, the Th ions interact with the central arene in a η^6-fashion, with Th-C$_{centroid}$ distances (**2$^{OtBu(DME)}$**: 2.364(8) Å and **2^{Ph}-crypt**: 2.3869(19) Å) significantly shorter than those found in **1^{OtBu}** and **1^{Ph}**, revealing a stronger interaction between the arene and the metal center. Moreover, the average arene C-C lengths of the arene anchor in **2$^{OtBu(DME)}$** (1.43 (2) Å) and in **2^{Ph}-crypt** (1.44(5) Å) are significantly

longer than those found in the precursor **1^{OtBu}** (1.400(6) Å), **1^{Ph}** (1.389(6) Å). The planarity of the central arene is significantly distorted in complex **2$^{OtBu(DME)}$** and **2^{Ph}-crypt** with maximum values of torsion angles at 21(2)° and 24.5(7)°, respectively, providing strong evidence of the presence of a reduced arene moiety. These values are consistent with a di-reduced arene bound to a Th(IV) center.[12a, 3c] Similar high torsion angles were also found in the analogous uranium [K(THF)U((OSi(O^{t}Bu)$_2$Ar)$_3$-arene)(THF)] (22.0(11)°)[14c] and cerium [K$_2$(Ce((OSi(O^{t}Bu)$_2$Ar)$_3$-arene)(Et$_2$O)$_2$] (18.0(11)°)[15a] complexes.

The reduction of the Th(IV) complex **1^{OtBu}** proceeds differently from what was reported for the reduction of the U(III) and Ce(III) complexes of the ($^-$OSi(O^{t}Bu)$_2$Ar)$_3$-arene ligand, which led first to the stabilization of the U(II) and Ce(II) analogues, followed by ligand-based reduction. Furthermore, the formation of a one-electron reduction product of the complexes **1^{OtBu}** and **1^{Ph}** could not be observed and two-electron reduction is the only product observed for the thorium complexes.

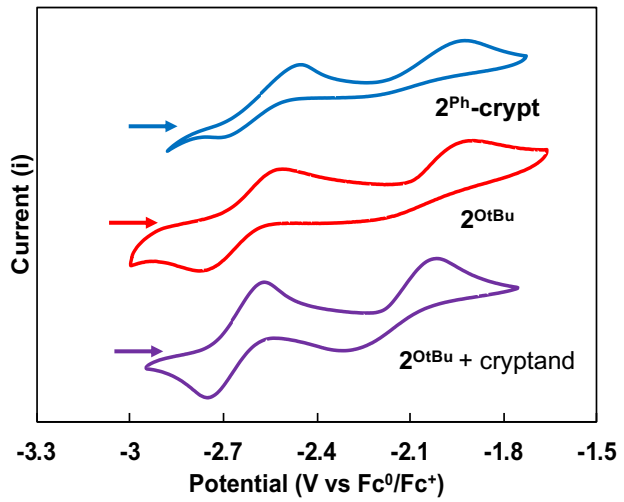

Figure 2. Cyclic voltammograms for complexes, **2^{OtBu}** (red) , **2^{Ph}-crypt** (blue) and **2^{OtBu}** + cryptand (purple) in THF. Conditions: Pt disk working electrode, referenced to the Fc^0/Fc$^+$ couple; 0.1 M [NBu$_4$][BPh$_4$] electrolyte in THF. Scan rate (250 mV/s). Arrows indicate the scan direction.

Cyclic voltammograms were measured for 3 mM THF solutions of complexes **2^{OtBu}** and **2^{Ph}-crypt**. The measurements were performed with 0.1 M [NBu$_4$][BPh$_4$] as the supporting electrolyte with decamethylferrocene (Fc*) as the internal reference (Figure 2).The cyclic voltammogram for complex **2^{OtBu}** in THF revealed two quasi reversible redox events at values of $E_{1/2}$ = -2.05, and -2.65 V vs. Fc$^{+/0}$ (Figure 2). The two measured waves display reduction events with E_{pc} values of -2.20 V and -2.78 V vs. Fc$^{+/0}$, respectively. These values are significantly more positive than the range of values reported for Th(IV)/Th(III) (-3.00 to -3.48 V vs. Fc$^{+/0}$), and Th(III)/Th(II) (-2.89 to -3.30 V vs. Fc$^{+/0}$), couples in complexes supported by Cp ligands [19] indicating these two redox events should be essentially ligand-based although some metal contribution cannot be ruled out. The voltammogram of **2^{OtBu}** after the addition of cryptand shows comparable E_{pc} values at -2.32 and -2.74 V vs. Fc$^{+/0}$, suggesting that the bound K$^+$ ion does not have significant effect on the reduction potentials. The di-reduced complex of the –OSiPh$_2$ substituted tripodal ligand, **2^{Ph}-crypt**, exhibits similar redox events, in which the two-reduction potentials for **2^{Ph}-crypt** (E_{pc} = -2.22 and -2.71 V vs. Fc$^{+/0}$) are comparable to those of **2^{OtBu}**. Overall, the cyclic voltammograms of the **2^{OtBu}** and **2^{Ph}-crypt** complexes show that both reduction events occur at the ligand in both complexes. Therefore, the different electron-donating character of the siloxide substituents (lower for the di(*tert*-butoxy) groups) does not significantly affect the redox properties of the two thorium complexes.

In order to gain some more insights on the nature of complexes **1^{OtBu}**, **1^{Ph}**, **2$^{OtBu(DME)}$** and **2^{Ph}-crypt**, DFT (B3PW91) calculations including dispersion corrections were carried out. The optimized geometries of the two Th(IV) precursors **1^{OtBu}** and **1^{Ph}** compares well with the experimental ones with a maximum deviation of 0.03 Å on the bond lengths around Th. As expected, the Th-Cl and Th-O bonds are found to be strongly polarized toward the hetero-element (Tables S5 and S16). In both cases, the HOMO is the arene π (the classical non-bonding one) while the LUMO is the π*(Tables S9 and S21). According to this, the reduction of complexes **1^{OtBu}** and **1^{Ph}** are anticipated to be ligand-based. To investigate if the reduction is ligand-based, complexes **2$^{OtBu(DME)}$** and **2^{Ph}-crypt** were optimized in two different spin states (namely singlet and triplet). For both complexes, the singlet is found to be the ground state with the triplet lying respectively 8.7 kcal.mol^{-1} and 10.7 kcal.mol^{-1} higher in energy(Tables S11 and S23). It is interesting to note that the optimized geometries of both singlet and triplet compare well with the experimental ones indicating that the Th is in a similar oxidation state in both spin state. This is further evidenced by comparing the Highest occupied Molecular Orbitals of the two spin states. In the singlet the HOMO is a doubly occupied δ-bonding interaction. Similarly, in the triplet state the two δ-bonding bonding orbitals are two singly occupied SOMOs. In the latter spin state, the unpaired spin density is mainly located in the arene ring (1.7 unpaired spin) so that one can safely conclude that the reduction is occurring at the arene rather than at the metal centre (see SI).

Based on the cyclic voltammetry studies of complexes **2^{OtBu}** and **2^{Ph}-crypt**, we assumed that these complexes can potentially transfer two-electrons to oxidizing substrates. Therefore, we set out to investigate the reactivity of complexes **2^{OtBu}** and **2^{Ph}-crypt** with selected substrates.

At first, we investigated the reaction with azobenzene (PhNNPh).

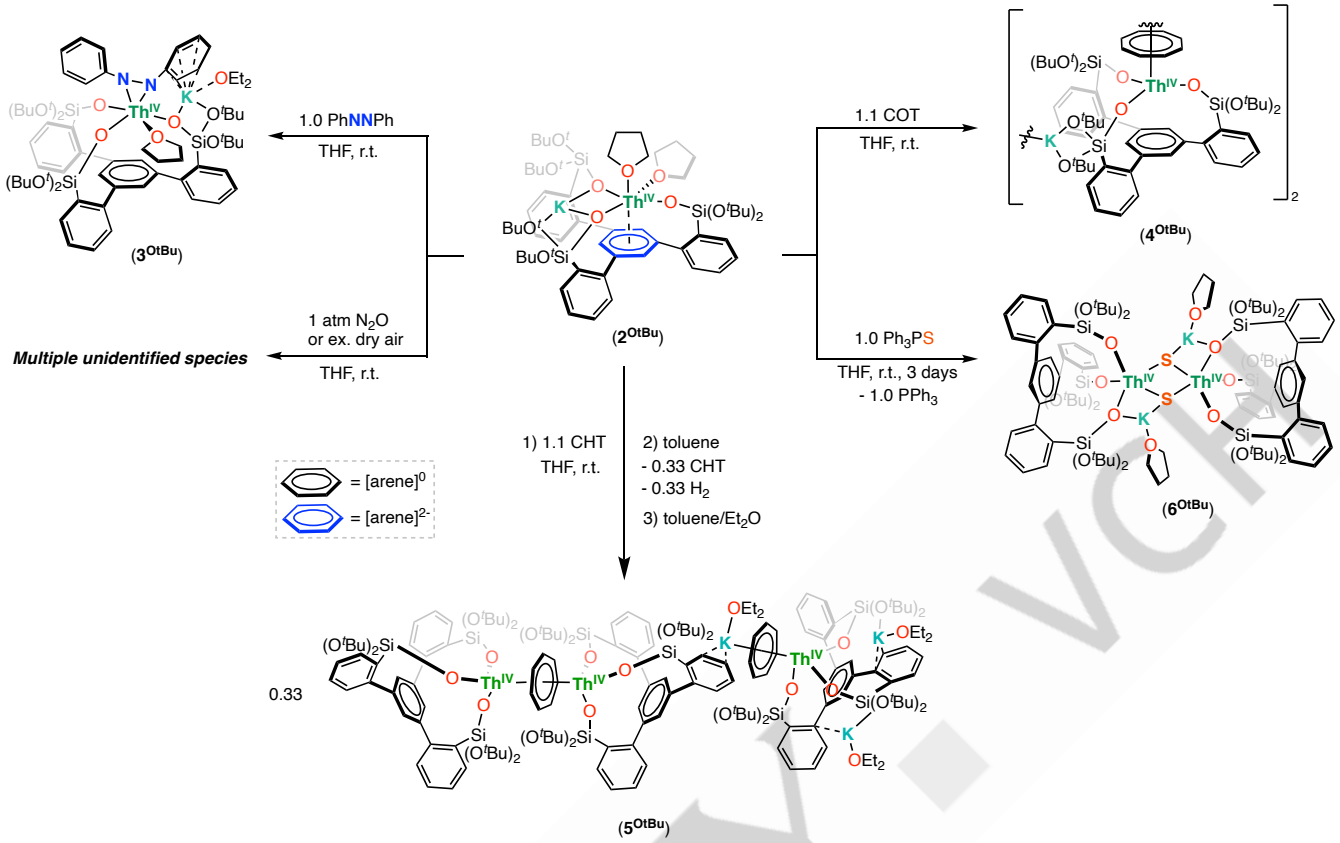

Scheme 2. Reactivity of complex **2**^{OtBu} towards small molecules.

The addition of 1.0 equiv. of PhNNPh to a solution of **2**^{OtBu} in THF led immediately to a color change from dark red-brown to yellow, full consumption of the starting material and formation of a new species as indicated by ^{1}H NMR spectroscopy (Figure S24-S25). Single crystals suitable for X-ray diffraction studies were obtained from Et_2O solution at -40 °C, and identified as the complex [K(Et_2O)Th((OSi(O^{t}Bu)$_2$Ar)$_3$-arene)(PhNNPh)(THF)] (**3**^{OtBu}) in 82% yield (Scheme 2). The solid-state molecular structure of complex **3**^{OtBu} (Figure 3) displays a mononuclear complex where the thorium cation is bound by three siloxide oxygens of the tripodal ligand and one [PhNNPh]$^{2-}$ ligand in a pseudo-octahedral geometry. A potassium cation is bound in the second coordination sphere by one phenyl ring of [PhNNPh]$^{2-}$, two oxygens of one –OSi(O^{t}Bu)$_2$ ligand arm, and one Et_2O molecule. The Th ion no longer interacts with the arene anchor, where the Th1-$C_{centroid}$ distance (3.7759(18) Å) is significantly elongated compared to the precursor (2.364(8) Å). The Th-$O_{siloxide}$ bond distances (2.217(4)-2.254(4) Å) are shorter compared to the complex **2**$^{OtBu(DME)}$ and are slightly longer than the monomeric unit in the previously reported U(IV) analogue, [K(Et_2O)U((OSi(O^{t}Bu)$_2$Ar)$_3$-arene)(PhNNPh)(THF)] (2.178(2)-2.203(2) Å)[20] in agreement with the difference in ionic radii of the two metals. The N1–N2 bond distance (1.468(7) Å) of the dianionic [PhNNPh]$^{2-}$ moiety and Th1–N bond distances (2.332(4) and 2.370(4) Å) are slightly longer compared to the average values found in the only Th(IV)-(PhNNPh)$^{2-}$ complex reported so far, [(NN^{TBS})Th-(THF)(PhNNPh)]$_2$ (NN^{TBS} = fc-(NSi^{t}BuMe$_2$)$_2$, fc = 1,1'-ferrocenediyl)](N-N: 1.466(7) Å and Th-N: 2.306(14Å)[12o]. The N1–N2 bond length (1.468(7) Å) is similar to that reported for dianionic compound, [K(18C6)]$_2$[PhNNPh] (1.40(3) Å),[20] and is elongated compared to neutral PhNNPh (1.25 Å) and to the singly reduced species, [K(2.2.2-cryptand)][PhNNPh] (1.34(3) Å),[1] compared to neutral PhNNPh (1.25 Å) and to the singly reduced species, [K(2.2.2-cryptand)][PhNNPh] (1.34(3) Å),[1] indicating

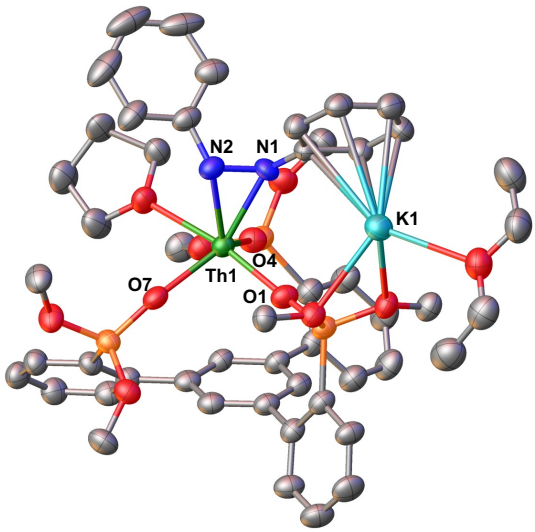

Figure 3. Molecular structure of [K(Et_2O)Th((OSi(O^{t}Bu)$_2$Ar)$_3$-arene)(PhNNPh)(THF)] (**3**^{OtBu}) with thermal ellipsoids at drawn at the 50% probability level. Hydrogen atoms and methyl groups on the –OSi(O^{t}Bu)$_2$ ligands have been omitted for clarity

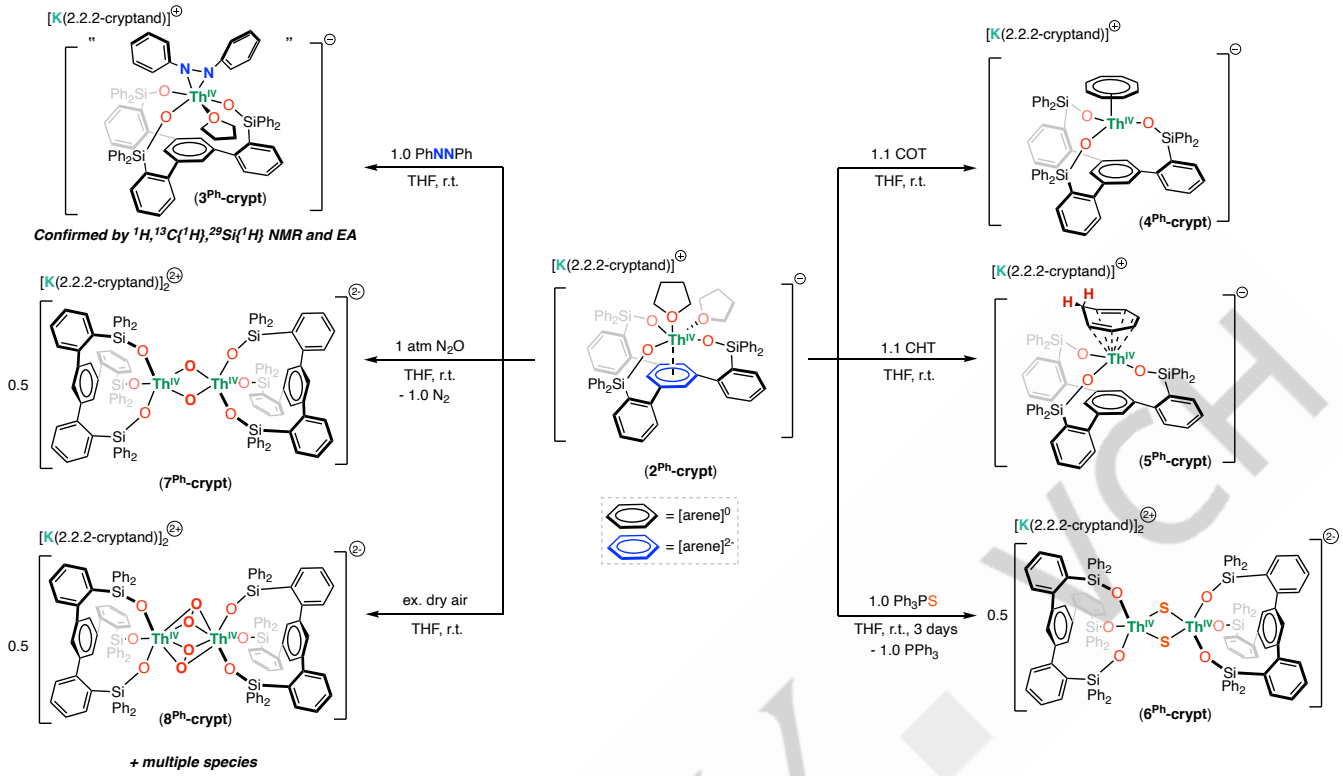

Scheme 3. Reactivity of complex **2^{Ph}-crypt** towards small molecules.

that complex **3^{OtBu}** has transferred two-electrons to the azobenzene to yield a dianionic $[PhNNPh]^{2-}$.

Complex **2^{Ph}-crypt** showed the same reactivity with azobenzene as **2^{OtBu}**, also resulting in the formation of the azobenzene adduct, [K(2.2.2-cryptand)][Th((OSiPh$_2$Ar)$_3$-arene)(PhNNPh)(THF)](**3^{Ph}-crypt**)(Scheme 3). Attempts to isolate single crystals for XRD analysis were not successful, but ^{1}H, ^{13}C{^{1}H}, ^{29}Si{^{1}H} NMR spectra and elemental analysis (See SI) are in agreement with the formation of **3^{Ph}-crypt**.

We also explored the reactivity of **2^{OtBu}** and **2^{Ph}-crypt** toward the potential two-electron acceptors cyclooctatetraene (COT, C_8H_8). Addition of 1.1 equiv. of COT to a solution of **2^{OtBu}** in THF resulted in the full consumption of **2^{OtBu}** and the formation of new resonances in the ^{1}H NMR spectrum (Figure S32-33). Colorless crystals were isolated from a concentrated toluene reaction mixture at room temperature and identified as the complex, [KTh((OSi(O^{t}Bu)$_2$Ar)$_3$-arene)(η^8-C_8H_8)]$_2$ (**4^{OtBu}**), in 70% yield (Scheme 2). Complex **2^{Ph}-crypt** also reacted with 1.1 equiv. of COT, leading to the formation of [K(2.2.2-cryptand][Th(OSiPh$_2$Ar)$_3$-arene)(η^8-C_8H_8)] (**4^{Ph}-crypt**) complex in 71% yield (Scheme 3 and See SI). The solid-state molecular structure of complex **4^{OtBu}** (Figure 4 and Figure S62) displays the presence of a dimeric bimetallic structure where two [KTh((OSi(O^{t}Bu)$_2$Ar)$_3$-arene)(η^8-C_8H_8)] moieties are held together by the K$^+$ cations bridging the two oxygens of one –OSi(O^{t}Bu)$_2$ arm and a COT^{2-} dianion. The Th ion no longer interacts with the distorted arene anchor, where the Th1-$C_{centroid}$ distance (4.143(2) Å) is significantly elongated compared to the precursor (2.364(8)

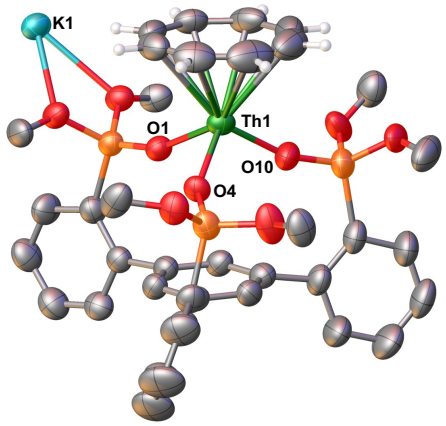

Figure 4. Molecular structure of monomeric unit of [KTh((OSi(O^{t}Bu)$_2$Ar)$_3$-arene)(η^8-C_8H_8)]$_2$ in **4^{OtBu}** with thermal ellipsoids at drawn at the 50% probability level. Hydrogen atoms, and methyl groups on the –OSi(O^{t}Bu)$_2$ ligands have been omitted for clarity.

Å). The planar COT^{2-} moiety binds in an η^8-fashion, where all C-C bond lengths in COT^{2-} (1.369(14)-1.426(10) Å) are consistent with the previous reported dianionic COT complex of thorium, [(NN^{TBS})Th-(THF)(η^8-COT)] (NN^{TBS} = fc-(NSi^{i}BuMe$_2$)$_2$, fc = 1,1'-ferrocenediyl)] (C-C_{COT} (1.384(16)-1.428(15) Å), Th1-$COT_{centroid}$ (2.103(3) Å) and Th1-C_{COT} (2.762(8)-2.809(9) Å).[12o] However, the Th1-C_{COT} (2.818(6)-2.876(9) Å) and Th1-$COT_{centroid}$ (2.174(3) Å) bond distances are slightly longer due to the presence of K$^+$ binding to COT^{2-}.

The solid-state molecular structure of complex **4^{Ph}-crypt** (Figure S63) shows the presence of an anionic mononuclear complex, [Th(OSiPh$_2$Ar)$_3$-arene)(η^8-C$_8$H$_8$)]$^-$ with the planar COT^{2-} moiety binding in an η^8-fashion. The structure is completed by one outer-sphere [K(2.2.2-cryptand]$^+$ cation. The C-C$_{COT}$ (1.380(17-1.445(17) Å), Th1-C$_{COT}$ (2.772(11)-2.816(10) Å) and Th1-COT$_{centroid}$ (2.099(4) Å) bond lengths are comparable to those found in **4^{OtBu}**. The geometrical parameters found for the complexes **4^{OtBu}** and **4^{Ph}-crypt** clearly indicates that complex **2^{OtBu}** and **2^{Ph}-crypt** act as two-electron reductants toward the COT substrate while retaining the precursor ligand framework.

We then explored the reactivity of **2^{OtBu}** and **2^{Ph}-crypt** with substrates, such as cycloheptatriene (CHT, C$_7$H$_8$), which can act as either a two-electron or three-electron acceptor.[21, 3c, 14c] Upon undergoing a two-electron reduction, C$_7$H$_8$ yields a C$_7$H$_8^{2-}$ dianion that adopts a non-planar geometry, coordinating to the metal in an η^6-fashion. When the C$_7$H$_8$ undergoes a three-electron reduction and subsequently undergoes H$_2$ elimination, cycloheptatriene achieves aromaticity, resulting in the formation of the planar C$_7$H$_7^{3-}$ anion.[21] It is noteworthy that actinide analogs containing CHT in its dianionic (C$_7$H$_8^{2-}$) and trianionic (C$_7$H$_7^{3-}$) form still remain rare.[23, 3c]

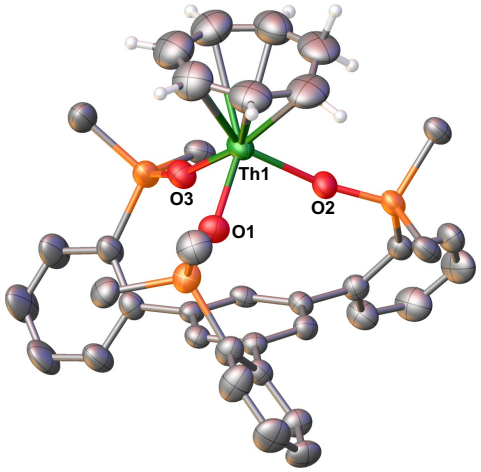

Figure 5. Molecular structure of anion [Th(OSiPh$_2$Ar)$_3$-arene(η^6-C$_7$H$_8$)]$^-$ in (**5^{Ph}-crypt**) with thermal ellipsoids at drawn at the 50% probability level. Hydrogen atoms, five carbon atoms of each Ph group on the –OSiPh$_2$ ligands and [K(2.2.2-cryptand)]$^+$ have been omitted for clarity.

The reactivity of both **2^{Ph}-crypt** and **2^{OtBu}** with CHT were examined. The addition of 1.1 equiv. of CHT to a THF solution of **2^{Ph}-crypt** resulted in a color change from dark purple to dark green and full consumption of the starting material to yield a new species as indicated by ^{1}H NMR studies after 1 hour at room temperature (Figure S46). Single crystals suitable for X-ray diffraction studies were obtained from a mixture of toluene and THF at room temperature and identified as [K(2.2.2-cryptand)][Th(OSiPh$_2$Ar)$_3$-arene(η^6-C$_7$H$_8$)] (**5^{Ph}-crypt**), in 73% yield (Scheme 3). The ^{1}H NMR spectrum of **5^{Ph}-crypt** in THF-d_8 showed five distinct resonances at δ 4.98, 4.34, 3.50, 0.50 and -1.87 ppm, which can be assigned to the bound η^6-C$_7$H$_8^{2-}$ (Figure S47). The solid-state molecular structure for complex **5^{Ph}-crypt** (Figure 5) displays an anionic mononuclear Th(IV) complex, [Th(OSiPh$_2$Ar)$_3$-arene(η^6-C$_7$H$_8$)]$^-$ and an outer-sphere [K(2.2.2-cryptand)]$^+$ cation. The Th1-O$_{siloxide}$ bond distances (2.215(3)-2.226(3) Å) are slightly shorter than those found in the precursor, **2^{Ph}-crypt** (2.257(3)-2.298(3) Å). The Th ion no longer interacts with the arene anchor, where the Th1-C$_{centroid}$ distance (4.2136(15) Å) is significantly elongated compared to the precursor (2.3869(19) Å). The CHT moiety adopts a terminal η^6 binding mode, with two C-C$_{CHT}$ bond lengths being elongated (C68-C74: 1.460(15) and C68-C69: 1.499(15) Å) compared to the five remaining bonds (1.364(15)-1.449(18) Å). These bond lengths are slightly longer and shorter when compared to free CHT (where C=C: 1.356 Å; C–C: 1.446 Å; CH–CH2: 1.505 Å)[22] and are consistent with the only reported uranium analogue containing the η^6-C$_7$H$_8^{2-}$ moiety, [K(Et$_2$O)U((OSi(O^{t}Bu)$_2$Ar)$_3$-arene)(η^6-C$_7$H$_8$)].[14c]

The reaction of **2^{OtBu}** with 1.1 equiv. of CHT in THF proceeds similarly leading immediately to a color change from dark red-brown to brown. The ^{1}H NMR spectrum of the reaction mixture revealed the presence of [KTh((OSi(O^{t}Bu)$_2$Ar)$_3$-arene)(η^6-C$_7$H$_8$)], displaying five resonances at δ 5.91, 5.03, 4.07, and -0.93 ppm (with one resonance overlapping with the other signals), which corresponds to the bound η^6-C$_7$H$_8^{2-}$(Figure S40). However, dissolution of the reaction mixture (after drying) in toluene resulted in a gradual change of the ^{1}H NMR spectrum (Figure S41-42) and led to observation of free CHT release which was not observed for the **2^{Ph}-crypt** complex. Single crystals suitable for X-ray diffraction studies were obtained from a concentrated toluene/Et$_2$O solution at -40°C in the absence of cryptand in 59% yield and identified as the trimeric complex, [K(Et$_2$O)$_3$(Th((OSi(O^{t}Bu)$_2$Ar)$_3$-arene)$_2$(μ-η^7,η^7 C$_7$H$_7$)(Th((OSi(O^{t}Bu)$_2$Ar)$_3$-arene)(η^7-C$_7$H$_7$)] (**5^{OtBu}**) (Scheme 2).

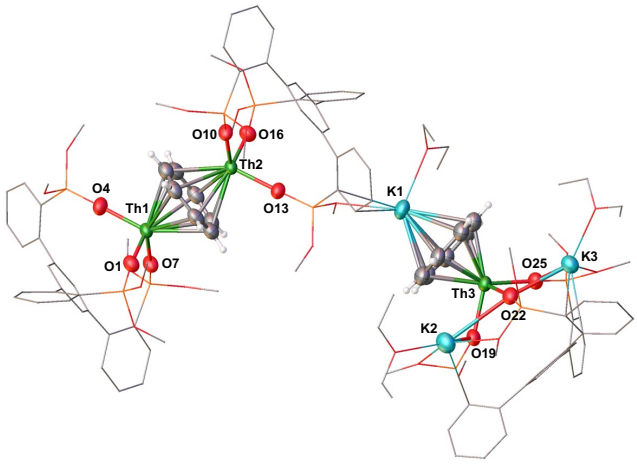

Figure 6. Molecular structure of [K(Et$_2$O)$_3$(Th((OSi(O^{t}Bu)$_2$Ar)$_3$-arene)$_2$(μ-η^7,η^7-C$_7$H$_7$)(Th((OSi(O^{t}Bu)$_2$Ar)$_3$-arene)(η^7-C$_7$H$_7$)] (**5^{OtBu}**) with tripodal moieties depicted as wire frames for clarity. Thermal ellipsoids at drawn at the 50% probability level. Hydrogen atoms and methyl groups on the –OSi(O^{t}Bu)$_2$ ligands have been omitted for clarity.

The molecular structure of complex **5^{OtBu}** (Figure 6) shows the presence of three [Th((OSi(O^{t}Bu)$_2$Ar)$_3$-arene]$^+$ complexes, three K$^+$ ions and two trianionic $C_7H_7^{3-}$ groups where one trianionic $C_7H_7^{3-}$ moiety bridges two thorium centers while a potassium cation bridges the resulting dimer to the trianionic $C_7H_7^{3-}$ moiety terminally bound to a mononuclear thorium complex [Th((OSi(O^{t}Bu)$_2$Ar)$_3$-arene]$^+$. The planar $C_7H_7^{3-}$ moiety binds in an η^7-fashion, where all C-C$_{CHT}$ (1.34(2)-1.48(2) Å), Th-C$_{CHT}$ bond lengths (2.584(16)-2.840(14) Å) and Th-CHT$_{centroid}$ distance (2.082(7)-2.284(16) Å) are longer than those found in the reported tripodal uranium analogue, [(K(Et$_2$O))$_2$)U((OSi(O^{t}Bu)$_2$Ar)$_3$-arene)(η^7-C$_7$H$_7$)$_\infty$ [14c] and in the three uranium complexes of trianionic CHT (η^7-$C_7H_7^{3-}$) previously reported.[23, 3c] This elongation is attributed to the slightly larger ionic radius of thorium. The Th ions no longer interact with the arene anchor, where the Th-C$_{centroid}$ distances (4.124(6)-4.361(6) Å) are significantly elongated compared to the di-reduced precursor (2.364(8) Å). The ^{1}H NMR spectrum of **5^{OtBu}** in THF-d_8 shows two distinct resonances at δ 5.61 and 4.86 ppm (Figure S43) that were attributed to the two different aromatic trianionic $C_7H_7^{3-}$ species.

The formation of **5^{OtBu}** in toluene is the result of the release of a neutral CHT ligand (observed by ^{1}H NMR) from a putative mononuclear (η^6-C_7H_8)$^{2-}$ complex analogue of **5^{Ph}-crypt** and only occurs in the presence of the potassium counterion.

Notably, release of CHT in toluene was prevented by addition of 2.2.2-cryptand to the **2^{OtBu}** (Figure S43) but did not allow isolation of the mononuclear (η^6-C_7H_8)$^{2-}$ complex in crystalline form.

To the best of our knowledge, complexes **5^{OtBu}** and **5^{Ph}-crypt** represent the first examples of thorium CHT adducts featuring η^7-$C_7H_7^{3-}$ and η^6-$C_7H_8^{2-}$ moieties, respectively. Moreover, the formation of **5^{OtBu}** and **5^{Ph}-crypt** clearly indicate that both **2^{OtBu}** and **2^{Ph}-crypt** behave as two-electron reductants in the reaction with CHT despite the different product formed.

Furthermore, we investigated the possibility of accessing terminal or bridging sulfides, which remain extremely rare in thorium chemistry[24], from the reaction of **2^{OtBu}** and **2^{Ph}-crypt** with the two-electron oxidizing reagent, triphenylphosphine sulfide (Ph$_3$PS).

The reaction of 1.0 equiv. of Ph$_3$PS with a THF solution of complex **2^{OtBu}** at room temperature for 3 days, resulted in a pink suspension. The ^{1}H NMR spectrum of the reaction mixture showed the full consumption of the starting material and the newly formed species precipitated from the solution (Figure S51). Single crystals suitable for X-ray diffraction studies were obtained from a diluted THF solution at room temperature and were identified as the dimeric complex, [(K(THF)Th((OSi(O^{t}Bu)$_2$Ar)$_3$-arene))$_2$(μ-S)$_2$] (**6^{OtBu}**) in 91% yield (Scheme 2).

The solid-state structure of **6^{OtBu}** (Figure 7) shows the presence of a dinuclear complex consisting of two equivalent Th(IV) moieties, bridged by two sulfide ligands. Each thorium center is penta-coordinated in a distorted square-pyramidal geometry and is bound by three –OSi(O^{t}Bu)$_2$ arms and the two bridging sulfides. Two K$^+$ cations are bound by two –OSi(O^{t}Bu)$_2$ arms and one THF molecule. The Th-S distances (2.725(5)-2.755(4) Å) are longer than the only two reported examples of the Th sulfide dimers supported by cyclopentadienyl ligands, [(η^5-1,2,4-(Me$_3$C)$_3$C$_5$H$_2$)$_2$Th)$_2$(μ-S)$_2$] (2.713(2)-2.726(2) Å)[25] and [η^5-1,3-(Me$_3$C)$_2$C$_5$H$_3$)$_2$Th)$_2$(μ-S)$_2$] (2.668(1) Å)[26]. The Th-S-Th angles are equivalent in **6^{OtBu}**, with values of 99.31(12)° and are in line with those reported for the bis-sulfide Th(IV) complexes supported by Cp ligands (95.65(4)-103.45(6)°).[26][25] The reactivity of **2^{Ph}-crypt** with Ph$_3$PS was also examined. The reaction of 1.0 equiv. of Ph$_3$PS with a THF solution of complex **2^{Ph}-crypt** at room temperature for 3 days, resulted in a dark green solution. Single crystals suitable for X-ray diffraction studies were obtained from a concentrated THF/toluene solution at room temperature and were identified as the dimeric complex, [K(2.2.2-cryptand]$_2$[Th((OSiPh$_2$Ar)$_3$-arene)]$_2$(μ-S)$_2$] (**6^{Ph}-crypt**) in 52% yield (Scheme 3).

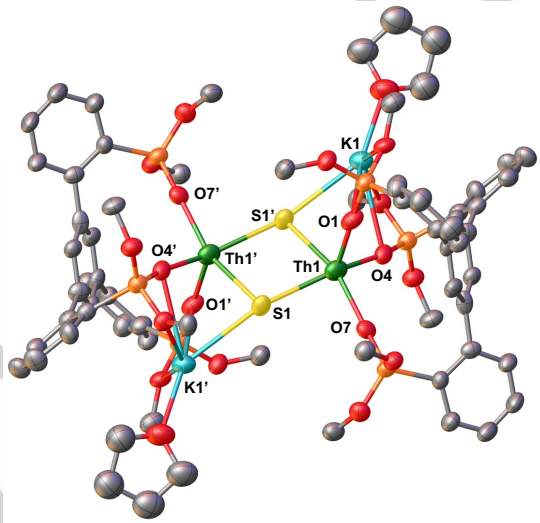

Figure 7. Molecular structure of [(K(THF)Th((OSi(O^{t}Bu)$_2$Ar)$_3$-arene))$_2$(μ-S)$_2$] (**6^{OtBu}**) with thermal ellipsoids at drawn at the 50% probability level. Hydrogen atoms and methyl groups on the –OSi(O^{t}Bu)$_2$ ligands have been omitted for clarity.

The solid structure of **6^{Ph}-crypt** (Figure S65) was found to be very similar to tert-butoxy analogue (**6^{OtBu}**), with two outer-sphere [K(2.2.2-cryptand)] cations instead of bound K$^+$ cations in the structure.

Additionally, the Th-S distances (2.706(2)-2.785(2) Å) are similar to those observed in **6^{OtBu}**, but Th-S-Th angles (96.73(10)-97.54(10)°) are slightly smaller than those observed in **6^{OtBu}** due to the absence of bound K$^+$ ions. Notably, in both cases, the Th ions no longer interact with the arene anchor, where the Th-C$_{centroid}$ distances (4.072(6)-4.1294(4) Å) are significantly elongated compared to the di-reduced precursors (2.364(8)-2.3869(19) Å). The reactions of **2^{OtBu}** and **2^{Ph}-crypt** with Ph$_3$PS most likely proceed with the two-electron reduction of Ph$_3$PS and formation of terminal Th(IV) sulfides that rapidly dimerize. Dimerization of Th(IV) sulfides due to their high basicity has been reported[24a] and is only prevented by tuning the sterics of supporting ligands.

Finally, we investigated the ability of **2^{OtBu}** and **2^{Ph}-crypt** of transferring two electrons to oxo transfer agents yielding rare Th

oxo complexes. The isolation of thorium oxo complexes remain limited to few examples of terminal [24a, 27, 10n] or bridging[24a, 26, 13] oxo complexes which include a very recent example supported by a redox active ligand.[10n] Common route to generate metal oxo compounds involves activation of dioxygen or using oxygen transfer reagents such as N_2O. However, the examples of well characterized products isolated from the reaction of actinide complexes with dioxygen remains extremely limited, mainly due to the uncontrollable formation of insoluble oxo byproducts.[28, 10n].

At first, we examined the reaction with strong oxidizing agent N_2O. Addition of excess N_2O (1 atm) to a THF solution of **2^{OtBu}** led immediately to a color change from dark red-brown to pink and to the formation of multiple products as indicated by ^{1}H NMR spectroscopy (Figure S56). Attempts to isolate XRD quality crystals proved unsuccessful.

Interestingly, the addition of an excess of N_2O (1 atm) to a THF solution of **2^{Ph}-crypt** immediately led to a color change from dark purple to colorless, resulting in the full consumption of the **2^{Ph}-crypt** and appearance of a single new species, as indicated by the ^{1}H NMR spectrum (Figure S57). Single crystals suitable for X-ray diffraction studies were obtained in 67% yield from a concentrated THF solution at room temperature and were identified as the dimeric complex, [K(2.2.2-cryptand)]$_2$[Th((OSiPh$_2$Ar)$_3$-arene)$_2$(μ-O)$_2$(THF)] (**7^{Ph}-crypt**) (Scheme 3).

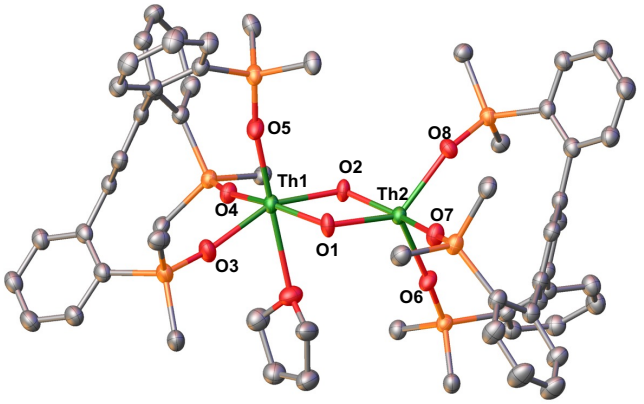

Figure 8. Molecular structure of dianion [(Th((OSiPh$_2$Ar)$_3$-arene))$_2$(μ-O)$_2$(THF)]$^{2-}$ in (**7^{Ph}-crypt**) with thermal ellipsoids at drawn at the 50% probability level. Hydrogen atoms, five carbon atoms of each Ph group on the –OSiPh$_2$ ligands and [K(2.2.2-cryptand)]$_2^{2+}$ have been omitted for clarity.

The molecular structure of **7^{Ph}-crypt** (Figure 8) shows the presence of a dinuclear complex consisting of two equivalent Th(IV) complexes, bridged by two oxide ligands. The two Th-O$_{oxo}$ distances (2.1850(17)-2.2109(17) Å) are in the range of those found in other reported oxo bridged Th(IV)(μ-O)$_2$ complexes (2.135(9)-2.203(4) Å)[24a, 26, 13] but significantly longer than the Th-O distances found in terminal Th-oxo complexes (1.983(7) Å-2.209 (4) Å).[24a] [27, 10n] The Th-O-Th angles (106.56(8)-106.63(8)°) are in line with those reported for the bis-oxide Th(IV) complexes supported by –OSi(O^{t}Bu)$_3$ and Cp ligands (106.1(4)-108.9(2) °).[24a, 26, 13] Moreover, the Th ions no longer interact with the arene anchor, where the Th-C$_{centroid}$ distance (4.2125(12)-4.2336(11) Å) are significantly elongated compared to the di-reduced precursor (2.3869(19) Å). The different reactivity of N_2O may be attributed to the bulky tripodal ligand environment in **2^{OtBu}**, which disfavored the dimerization of reactive Th(IV) terminal oxo intermediates.

Next, we pursued the reactivity of **2^{OtBu}** and **2^{Ph}-crypt** with dioxygen from dry air. Addition of excess dry air to a THF solution of **2^{OtBu}** and **2^{Ph}-crypt**, resulted in a colorless solution immediately, indicating the oxidation occurred. Analysis by ^{1}H NMR spectroscopy showed the presence of multiple species in both cases (Figure S61-S62). Attempt to isolate single crystals suitable for XRD analysis were unsuccessful for the oxidation products of **2^{OtBu}**. However, only a few single crystals suitable for X-ray diffraction studies were obtained from a concentrated THF solution at room temperature from the oxidation of **2^{Ph}-crypt** and identified as the dimeric complexes, [K(2.2.2-cryptand)]$_2$[Th((OSiPh$_2$Ar)$_3$-arene)]$_2$(μ-η^2:η^2-O$_2$)$_2$(THF)] (**8^{Ph}-crypt**)(Scheme 3 and Figure 9). Attempts to isolate analytically pure complex **8^{Ph}-crypt** by changing temperature and stoichiometric conditions proved unsuccessful due to the formation of multiple unidentified products.

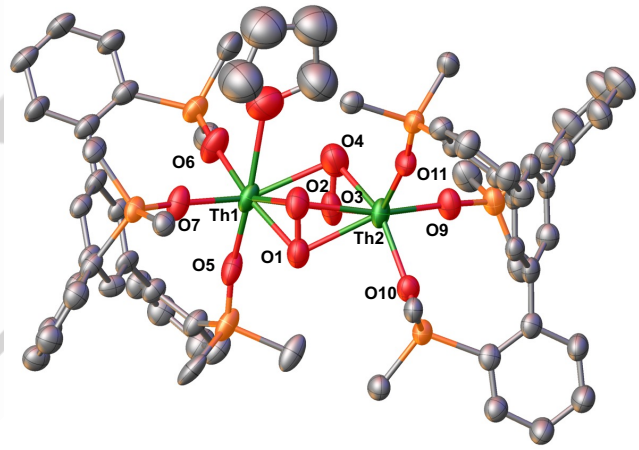

Figure 9. Molecular structure of dianion [(Th((OSiPh$_2$Ar)$_3$-arene))$_2$(μ-η^2:η^2-O$_2$)$_2$(THF)]$^{2-}$ in (**8^{Ph}-crypt**) with thermal ellipsoids at drawn at the 50% probability level. Hydrogen atoms, five carbon atoms of each Ph group on the –OSiPh$_2$ ligands and [K(2.2.2-cryptand)]$_2^{2+}$ have been omitted for clarity.

Conclusion

In summary, we reported the synthesis and the redox reactivity of two Th(IV) complexes supported by arene-tethered tris(siloxide) tripodal ligands [(KOSiR$_2$Ar)$_3$-arene)]. The two- electron reduction of these Th(IV) complexes generates the di-reduced [KTh((OSi(O^{t}Bu)$_2$Ar)$_3$-arene)(THF)$_2$] (**2^{OtBu}**) and [K(2.2.2-cryptand)][Th(OSiPh$_2$Ar)$_3$-arene)(THF)$_2$](**2^{Ph}-crypt**) where the formal oxidation state of Th is +II. Structural and computational studies indicate that the reduction occurred at the arene anchor of the ligand. The robust tripodal frameworks stores two electrons in the arene anchor, which become available at the metal center for the controlled two-electron reduction of a broad range of substrates (N_2O, COT, CHT, Ph_2N_2, Ph_3PS and O_2) while the

ligand framework is retained in its original form. We found that the presence of substituents with different electron-donating properties (tert-butoxy vs phenyl groups) on the siloxide arms of the tripodal ligand does not significantly affect the redox reactivity of the Th complexes probably because the electrons are localized on the arene anchor. However, changing the nature of the substituents can facilitate the isolation of the reaction products and we found that the phenyl substituents allow the isolation of an unprecedented thorium peroxide bridged complex. This work shows that arene-tethered tris(siloxide) tripodal ligands allow implementation of two-electron redox chemistry at the thorium center while retaining the ligand framework unchanged. These results open new perspectives in the chemistry of thorium.

Acknowledgements

We acknowledge support from the Swiss National Science Foundation grant number 200020_212723 and the Ecole Polytechnique Fédérale de Lausanne (EPFL).

Conflicts of interest

The authors declare no conflict of interest.

Keywords: thorium • redox-active ligands • tripodal ligands • actinides • redox reactivity

[1] L. Barluzzi, S. R. Giblin, A. Mansikkamaki, R. A. Layfield, *J. Am. Chem. Soc.* **2022**, *144*, 18229-18233.

[2] a) M. R. MacDonald, M. E. Fieser, J. E. Bates, J. W. Ziller, F. Furche, W. J. Evans, *J. Am. Chem. Soc.* **2013**, *135*, 13310-13313; b) C. J. Windorff, M. R. MacDonald, K. R. Meihaus, J. W. Ziller, J. R. Long, W. J. Evans, *Chem. Eur. J.* **2016**, *22*, 772-782; c) D. N. Huh, J. W. Ziller, W. J. Evans, *Inorg. Chem.* **2018**, *57*, 11809-11814; d) A. J. Ryan, M. A. Angadol, J. W. Ziller, W. J. Evans, *Chem. Commun.* **2019**, *55*, 2325-2327; e) F. S. Guo, N. Tsoureas, G. Z. Huang, M. L. Tong, A. Mansikkamaki, R. A. Layfield, *Angew. Chem. Int. Ed. Engl.* **2020**, *59*, 2299-2303.

[3] a) H. S. La Pierre, A. Scheurer, F. W. Heinemann, W. Hieringer, K. Meyer, *Angew. Chem. Int. Ed. Engl.* **2014**, *53*, 7158-7162; b) B. S. Billow, B. N. Livesay, C. C. Mokhtarzadeh, J. McCracken, M. P. Shores, J. M. Boncella, A. L. Odom, *J. Am. Chem. Soc.* **2018**, *140*, 17369-17373; c) M. D. Straub, E. T. Ouellette, M. A. Boreen, R. D. Britt, K. Chakarawet, I. Douair, C. A. Gould, L. Maron, I. Del Rosal, D. Villarreal, S. G. Minasian, J. Arnold, *J. Am. Chem. Soc.* **2021**, *143*, 19748-19760.

[4] a) D. S. J. Arney, C. J. Burns, *J. Am. Chem. Soc.* **1995**, *117*, 9448-9460; b) J. L. Kiplinger, D. E. Morris, B. L. Scott, C. J. Burns, *Chem. Commun.* **2002**, 30-31; c) S. Fortier, N. Kaltsoyannis, G. Wu, T. W. Hayton, *J. Am. Chem. Soc.* **2011**, *133*, 14224-14227; d) D. M. King, F. Tuna, E. J. L. McInnes, J. McMaster, W. Lewis, A. J. Blake, S. T. Liddle, *Science* **2012**, *337*, 717-720; e) J. L. Brown, S. Fortier, G. Wu, N. Kaltsoyannis, T. W. Hayton, *J. Am. Chem. Soc.* **2013**, *135*, 5352-5355; f) C. Camp, J. Pecaut, M. Mazzanti, *J. Am. Chem. Soc.* **2013**, *135*, 12101-12111; g) T. W. Hayton, *Chem.Commun.* **2013**, *49*, 2956-2973; h) A. J. Lewis, P. J. Carroll, E. J. Schelter, *J. Am. Chem. Soc.* **2013**, *135*, 511-518; i) C. Camp, M. A. Antunes, G. Garcia, I. Ciofini, I. C. Santos, J. Pecaut, M. Almeida, J. Marcalo, M. Mazzanti, *Chem. Sci.* **2014**, *5*, 841-846; j) E. L. Lu, O. J. Cooper, J. McMaster, F. Tuna, E. J. L. McInnes, W. Lewis, A. J. Blake, S. T. Liddle, *Angew. Chem. Int. Ed. Engl.* **2014**, *53*, 6696-6700; k) D. P. Halter, F. W. Heinemann, J. Bachmann, K. Meyer, *Nature* **2016**, *530*, 317-321; l) N. Tsoureas, A. F. R. Kilpatrick, C. J. Inman, F. G. N. Cloke, *Chem. Sci.* **2016**, *7*, 4624-4632; m) B. M. Gardner, C. E. Kefalidis, E. Lu, D. Patel, E. J. L. McInnes, F. Tuna, A. J. Wooles, L. Maron, S. T. Liddle, *Nat. Commun.* **2017**, 8, 1898; n) N. S. Settineri, A. A. Shiau, J. Arnold, *Chem. Commun.* **2018**, *54*, 10913-10916; o) N. T. Rice, K. McCabe, J. Bacsa, L. Maron, H. S. La Pierre, *J. Am. Chem. Soc.* **2020**, *142*, 7368-7373; p) R. J. Ward, P. Rungthanaphatsophon, I. del Rosal, S. P. Kelley, L. Maron, J. R. Walensky, *Chem. Sci.* **2020**, *11*, 5830-5835; q) D. K. Modder, C. T. Palumbo, I. Douair, R. Scopelliti, L. Maron, M. Mazzanti, *Chem. Sci.* **2021**, *12*, 6153-6158.

[5] M. Falcone, L. Chatelain, R. Scopelliti, I. Zivkovic, M. Mazzanti, *Nature* **2017**, *547*, 332-335.

[6] a) O. Cooper, C. Camp, J. Pécaut, C. E. Kefalidis, L. Maron, S. Gambarelli, M. Mazzanti, *J. Am. Chem. Soc.* **2014**, *136*, 6716-6723; b) L. Barluzzi, M. Falcone, M. Mazzanti, *Chem. Commun.* **2019**, *55*, 13031-13047; c) M. Falcone, L. Barluzzi, J. Andrez, F. F. Tirani, I. Zivkovic, A. Fabrizio, C. Corminboeuf, K. Severin, M. Mazzanti, *Nat. Chem.* **2019**, *11*, 154-160; d) D. R. Hartline, K. Meyer, *Jacs Au* **2021**, *1*, 698-709.

[7] a) M. S. Eisen, *Top. Organomet. Chem.* **2010**, *31*, 157-184; b) K. A. Erickson, J. L. Kiplinger, *Acs Catalysis* **2017**, *7*, 4276-4280; c) H. Liu, T. Ghatak, M. S. Eisen, *Chem. Commun.* **2017**, *53*, 11278-11297; d) S. Saha, M. S. Eisen, *Acs Catalysis* **2019**, *9*, 5947-5956.

[8] a) J. S. Parry, F. G. N. Cloke, S. J. Goles, M. B. Hursthouse, *J. Am. Chem. Soc.* **1999**, *121*, 6867-6871; b) P. C. Blake, N. M. Edelstein, P. B. Hitchcock, W. K. Kot, M. F. Lappert, G. V. Shalimoff, S. Tian, *J. Organomet. Chem.* **2001**, *636*, 124-129; c) J. R. Walensky, R. L. Martin, J. W. Ziller, W. J. Evans, *Inorg. Chem.* **2010**, *49*, 10007-10012; d) N. A. Siladke, C. L. Webster, J. R. Walensky, M. K. Takase, J. W. Ziller, D. J. Grant, L. Gagliardi, W. J. Evans, *Organometallics* **2013**, *32*, 6522-6531; e) R. R. Langeslay, M. E. Fieser, J. W. Ziller, F. Furche, W. J. Evans, *Chem. Sci.* **2015**, *6*, 517-521; f) R. R. Langeslay, M. E. Fieser, J. W. Ziller, F. Furche, W. J. Evans, *J. Am. Chem. Soc.* **2016**, *138*, 4036-4045; g) A. Formanuik, A. M. Ariciu, F. Ortu, R. Beekmeyer, A. Kerridge, F. Tuna, E. J. L. McInnes, D. P. Mills, *Nat. Chem.* **2017**, *9*, 578-583; h) R. R. Langeslay, G. P. Chen, C. J. Windorff, A. K. Chan, J. W. Ziller, F. Furche, W. J. Evans, *J. Am. Chem. Soc.* **2017**, *139*, 3387-3398; i) D. N. Huh, S. Roy, J. W. Ziller, F. Furche, W. J. Evans, *J. Am. Chem. Soc.* **2019**, *141*, 12458-12463.

[9] a) J. C. Wedal, S. Bekoe, J. W. Zitter, F. Furche, W. J. Evans, *Dalton Trans.* **2019**, *48*, 16633-16640; b) J. C. Wedal, N. Cajiao, M. L. Neidig, W. J. Evans, *Chem. Commun.* **2022**, *58*, 5289-5291.

[10] a) E. J. Schelter, R. L. Wu, J. M. Veauthier, E. D. Bauer, C. H. Booth, R. K. Thomson, C. R. Graves, K. D. John, B. L. Scott, J. D. Thompson, D. E. Morris, J. L. Kiplinger, *Inorg. Chem.* **2010**, *49*, 1995-2007; b) A. Mrutu, C. L. Barnes, S. C. Bart, J. R. Walensky, *Eur. J. Inorg. Chem.* **2013**, *2013*, 4050-4055; c) W. S. Ren, W. W. Lukens, G. F. Zi, L. Maron, M. D. Walter, *Chem. Sci.* **2013**, *4*, 1168-1174; d) W. S. Ren, E. W. Zhou, B. Fang, G. H. Hou, G. F. Zi, D. C. Fang, M. D. Walter, *Angew. Chem. Int. Ed. Engl.* **2014**, *53*, 11310-11314; e) E. W. Zhou, W. S. Ren, G. H. Hou, G. F. Zi, D. C. Fang, M. D. Walter, *Organometallics* **2015**, *34*, 3637-3647; f) A. Formanuik, F. Ortu, R. Beekmeyer, A. Kerridge, R. W. Adams, D. P. Mills, *Dalton Trans.* **2016**, *45*, 2390-2393; g) A. Formanuik, F. Ortu, C. J. Inman, A. Kerridge, L. Castro, L. Maron, D. P. Mills, *Chem. Eur. J.* **2016**, *22*, 17976-17979; h) F. Ortu, A. Formanuik, J. R. Innes, D. P. Mills, *Dalton*

Trans. **2016**, *45*, 7537-7549; i) P. K. Yang, E. W. Zhou, B. Fang, G. H. Hou, G. F. Zi, M. D. Walter, *Organometallics* **2016**, *35*, 2129-2139; j) A. Formanuik, F. Ortu, J. J. Liu, L. E. Nodaraki, F. Tuna, A. Kerridge, D. P. Mills, *Chem. Eur. J.* **2017**, *23*, 2290-2293; k) C. C. Zhang, P. K. Yang, E. W. Zhou, X. B. Deng, G. F. Zi, M. D. Walter, *Organometallics* **2017**, *36*, 4525-4538; l) S. S. Galley, S. A. Pattenaude, D. Ray, C. A. Gaggioli, M. A. Whitefoot, Y. S. Qiao, R. F. Higgins, W. L. Nelson, R. Baumbach, J. M. Sperling, M. Zeller, T. S. Collins, E. J. Schelter, L. Gagliardi, T. E. Albrecht-Schonzart, S. C. Bart, *Inorg. Chem.* **2021**, *60*, 15242-15252; m) D. Rupasinghe, H. Gupta, M. R. Baxter, R. F. Higgins, M. Zeller, E. J. Schelter, S. C. Bart, *Inorg. Chem.* **2021**, *60*, 14302-14309; n) D. Rupasinghe, M. R. Baxter, H. Gupta, A. T. Poore, R. F. Higgins, M. Zeller, S. L. Tian, E. J. Schelter, S. C. Bart, *J. Am. Chem. Soc.* **2022,** *144,* 17423–17431.; o) S. S. Galley, R. Higgins, J. J. Kiernicki, L. M. Lopez, J. R. Walensky, E. J. Schelter, M. Zeller, S. C. Bart, *Inorg. Chem.* **2023**, *62*, 15819-15823.

[11] a) I. Korobkov, S. Gambarotta, G. P. A. Yap, *Angew. Chem. Int. Ed. Engl.* **2003**, *42*, 814-818; b) I. Korobkov, S. Gambarotta, *Organometallics* **2004**, *23*, 5379-5381.

[12] a) M. N. Bochkarev, *Chem. Rev.* **2002**, *102*, 2089-2117; b) D. P. Mills, F. Moro, J. McMaster, J. van Slageren, W. Lewis, A. J. Blake, S. T. Liddle, *Nat. Chem.* **2011**, *3*, 454-460; c) P. L. Arnold, S. M. Mansell, L. Maron, D. McKay, *Nat. Chem.* **2012**, *4*, 668-674; d) P. L. Arnold, J. H. Farnaby, R. C. White, N. Kaltsoyannis, M. G. Gardiner, J. B. Love, *Chem. Sci.* **2014**, *5*, 756-765; e) W. L. Huang, P. L. Diaconescu, *Dalton Trans.* **2015**, *44*, 15360-15371; f) C. M. Kotyk, M. E. Fieser, C. T. Palumbo, J. W. Ziller, L. E. Darago, J. R. Long, F. Furche, W. J. Evans, *Chem. Sci.* **2015**, *6*, 7267-7273; g) S. T. Liddle, *Coord. Chem. Rev.* **2015**, *293*, 211-227; h) M. E. Fieser, C. T. Palumbo, H. S. La Pierre, D. P. Halter, V. K. Voora, J. W. Ziller, F. Furche, K. Meyer, W. J. Evans, *Chem. Sci.* **2017**, *8*, 7424-7433; i) S. Fortier, J. R. Aguilar-Calderon, B. Vlaisavljevich, A. J. Metta-Magana, A. G. Goos, C. E. Botez, *Organometallics* **2017**, *36*, 4591-4599; j) C. J. Inman, A. S. P. Frey, A. F. R. Kilpatrick, F. G. N. Cloke, S. M. Roe, *Organometallics* **2017**, *36*, 4539-4545; k) M. Suvova, K. T. P. O'Brien, J. H. Famaby, J. B. Love, N. Kaltsoyannis, P. L. Arnold, *Organometallics* **2017**, *36*, 4669-4681; l) D. P. Halter, C. T. Palumbo, J. W. Ziller, M. Gembicky, A. L. Rheingold, W. J. Evans, K. Meyer, *J. Am. Chem. Soc.* **2018**, *140*, 2587-2594; m) M. Mazzanti, *Nat. Chem.* **2018**, *10*, 247-249; n) A. J. Wooles, D. P. Mills, F. Tuna, E. J. L. McInnes, G. T. W. Law, A. J. Fuller, F. Kremer, M. Ridgway, W. Lewis, L. Gagliardi, B. Vlaisavljevich, S. T. Liddle, *Nat. Commun.* **2018**, *9*, 2097 o) C. Yu, J. F. Liang, C. Deng, G. Lefevre, T. Cantat, P. L. Diaconescu, W. L. Huang, *J. Am. Chem. Soc.* **2020**, *142*, 21292-21297; p) J. Murillo, R. Bhowmick, K. L. M. Harriman, A. Gomez-Torres, J. Wright, R. W. Meulenberg, P. Miro, A. Metta-Magana, M. Murugesu, B. Vlaisavljevich, S. Fortier, *Chem. Sci.* **2021**, *12*, 13360-13372.

[13] F. C. Hsueh, T. Rajeshkumar, B. Kooij, R. Scopelliti, K. Severin, L. Maron, I. Zivkovic, M. Mazzanti, *Angew. Chem. Int. Ed. Engl.* **2023**, *62,* e202215846.

[14] a) D. P. Halter, F. W. Heinemann, L. Maron, K. Meyer, *Nat. Chem.* **2018**, *10*, 259-267; b) C. Deng, J. F. Liang, R. Sun, Y. Wang, P. X. Fu, B. W. Wang, S. Gao, W. L. Huang, *Nat. Commun.* **2023**, *14, 4657*; c) M. Keener, R. A. K. Shivaraam, T. Rajeshkumar, M. Tricoire, R. Scopelliti, I. Zivkovic, A. S. Chauvin, L. Maron, M. Mazzanti, *J. Am. Chem. Soc.* **2023**, *145*, 16271-16283.

[15] a) F. C. Hsueh, T. Rajeshkumar, L. Maron, R. Scopelliti, A. Sienkiewicz, M. Mazzanti, *Chem. Sci.* **2023**, *14*, 6011-6021; b) Y. Wang, J. F. Liang, C. Deng, R. Sun, P. X. Fu, B. W. Wang, S. Gao, W. L. Huang, *J. Am. Chem. Soc.* **2023,** *145*, 22466–22474.

[16] a) R. R. Thompson, M. E. Rotella, P. Du, X. Zhou, F. R. Fronczek, R. Kumar, O. Gutierrez, S. Lee, *Organometallics* **2019**, *38*, 4054-4059; b) J. Hillenbrand, M. Leutzsch, E. Yiannakas, C. P. Gordon, C. Wille, N. Nothling, C. Coperet, A. Furstner, *J. Am. Chem. Soc.* **2020**, *142*, 11279-11294.

[17] a) C. A. Cruz, D. J. H. Emslie, C. M. Robertson, L. E. Harrington, H. A. Jenkins, J. F. Britten, *Organometallics* **2009**, *28*, 1891-1899; b) I. Korobkov, B. Vidjayacoumar, S. I. Gorelsky, P. Billone, S. Gambarotta, *Organometallics* **2010**, *29*, 692-702; c) J. McKinven, G. S. Nichol, P. L. Arnold, *Dalton Trans.* **2014**, *43*, 17416-17421; d) F. Y. T. Lam, J. A. L. Wells, T. Ochiai, C. J. V. Halliday, K. N. McCabe, L. Maron, P. L. Arnold, *Inorg. Chem.* **2022**, *61*, 4581-4591.

[18] F. C. Hsueh, L. Barluzzi, M. Keener, T. Rajeshkumar, L. Maron, R. Scopelliti, M. Mazzanti, *J. Am. Chem. Soc.* **2022**, *144*, 3222-3232.

[19] J. C. Wedal, J. M. Barlow, J. W. Ziller, J. Y. Yang, W. J. Evans, *Chem. Sci.* **2021**, *12*, 8501-8511.

[20] R. A. K. Shivaraam, M. Keener, D. K. Modder, T. Rajeshkumar, I. Zivkovic, R. Scopelliti, L. MaronMaron, M. Mazzanti, *Angew. Chem. Int. Ed. Engl.* **2023**, *62*, e20230405.

[21] M. L. H. Green, D. K. P. Ng, *Chem. Rev.* **1995**, *95*, 439-473.

[22] M. Traetteberg, *J. Am. Chem. Soc.* **1964**, *86*, 4265-4270.

[23] a) T. Arliguie, M. Lance, M. Nierlich, J. Vigner, M. Ephritikhine, *J. Chem. Soc. Chem. Commun.* **1995**, 183-184; b) T. Arliguie, M. Lance, M. Nierlich, M. Ephritikhine, *J. Chem. Soc. Dalton Trans.* **1997**, 2501-2504.

[24] a) W. S. Ren, G. F. Zi, D. C. Fang, M. D. Walter, *J. Am. Chem. Soc.* **2011**, *133*, 13183-13196; b) M. A. Stuber, A. Y. Kornienko, T. J. Emge, J. G. Brennan, *Inorg. Chem.* **2017**, *56*, 10247-10256.

[25] C. C. Zhang, G. H. Hou, G. F. Zi, W. J. Ding, M. D. Walter, *J. Am. Chem. Soc.* **2018**, *140*, 14511-14525.

[26] C. C. Zhang, G. H. Hou, G. F. Zi, W. J. Ding, M. D. Walter, *Inorg. Chem.* **2019**, *58*, 1571-1590.

[27] D. E. Smiles, G. Wu, N. Kaltsoyannis, T. W. Hayton, *Chem. Sci.* **2015**, *6*, 3891-3899.

[28] L. Chatelain, V. Mougel, J. Pécaut, M. Mazzanti, *Chem. Sci.* **2012**, *3*, 1075-1079.

Entry for the Table of Contents

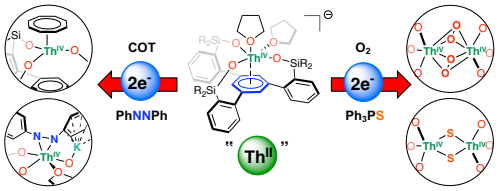

Two electrons can be stored by in the arene anchor of robust tripodal siloxide frameworks by chemical reduction of their Th(IV) complexes. The two electrons become available at the metal center for the controlled two-electron reduction of a broad range of substrates (N_2O, COT, CHT, Ph_2N_2, Ph_3PS and O_2) while the ligand framework is retained in its original form.

Institute and/or researcher Twitter usernames: @EPFL_CHEM_Tweet

@MazzantiLab